doi: 10.15407/ujpe61.10.0853

T. MAKHNII,[1] O. ILCHENKO,[1] A. REYNT,[1] Y. PILGUN,[2] A. KUTSYK,[2] D. KRASNENKOV,[1] M. IVASYUK,[3] V. KUKHARSKYY [1]

[1] D.F. Chebotarev State Institute of Gerontology of the NAMS of Ukraine
(67, Vyshhorodska Str., Kyiv 04114, Ukraine; e-mail: makhni1tanya@gmail.com)
[2] Faculty of Radio Physics, Electronics and Computer Systems,
Taras Shevchenko National University of Kyiv
(2, Prosp. Academician Glushkov, Kyiv 03022, Ukraine)
[3] Faculty of Life Science, National University of Kyiv-Mohyla Academy
(2, G. Skovoroda Str., Kyiv 04655, Ukraine)

PACS 78.30.C

AGE-RELATED CHANGES IN FTIR AND RAMAN SPECTRA OF HUMAN BLOOD

Blood analysis by spectroscopic techniques can provide important information about biochemistry and life processes in it. Blood indices are highly variable, and plenty of factors influence them. The present work describes the combination of two methods – IR and Raman spectroscopies of blood applied to investigate gerontology issues. We carried out a pilot study of 74 blood samples. The donors were differentiated by age with the Partial Least Squares (PLS) analysis of Raman and IR spectra. Analyzing the principal component spectra obtained during PLS processn the most illustrative bands were found in the intervals 2860–3030 cm^{-1}, 1370–1620 cm^{-1}, 1020–1220 cm^{-1} and in 1650–1530 cm^{-1}, 1380–1360 cm^{-1}, 1220–1200 cm^{-1}, 1002–1004 cm^{-1}, 760–750 cm^{-1} in IR and Raman spectral regions, respectively. Calibration models obtained via the PLS analysis of blood vibrational spectra provide the accuracy of age determination around ±15 years from FTIR data and around ±20 years from Raman data. Though such calibrations cannot be used for the precise determination of age, the age-related changes of blood do really exist and can be detected from vibrational spectra.

K e y w o r d s: human blood, age, Raman spectroscopy, ATR-FTIR spectroscopy, Partial Least Squares (PLS) analysis.

1. Introduction

IR and Raman spectroscopies are powerful tools for the investigation of chemical compounds [1, 2]. Recently, spectroscopic methods showed a huge potential for biomedical sciences [3]. A lot of scientific and diagnostic issues, which could be solved by spectroscopy, deal with providing a new information about the qualitative and quantitative compositions of biological samples. The major types of samples are body fluids (blood, urea, tears, *etc.*). Blood investigations show the simplicity, speed, and convenience of a research with the use of spectroscopy tools. The diagnostics makes it possible to distinguish healthy and diabetic bloods and to evaluate the hemoglobin level [4, 5]. It was shown that it is possible to achieve the differentiation of healthy and infected bloods close to 100%. Some research groups studied whole blood, while the other authors separated it into plasma, white blood cells, and red blood cells [6–9].

One of the important issues in biology could be also solved by spectroscopy – it is the age-related changes of body's indices. Some authors manage to correlate

spectral data and the age of donors [10, 11]. Age-related changes were found in UV Raman spectra (amide-I region) of human humerus bone [12].

The other way to use the vibrational spectroscopy, which could be applied to forensic science, is the age identification of a sample. It was shown that it is possible to discriminate between different body fluids by Raman spectra and to determine the donor age and specimen storage time for blood, saliva, and vaginal secretion by FTIR for crime investigations [13].

The other indispensable tool for such investigations is statistics. The mathematic analysis of the whole blood spectrum can provide a good classification between healthy and infected samples, normal and pathological glucose levels, and so on.

Statistical spectra analysis methods include the principle component analysis (PCA), partial least squares (PLS) analysis, discriminant analysis, *etc.* [14]. In our study, PLS was used to investigate age-related chemical alterations.

The main purpose of this work is to explore the possibility of using IR and Raman spectroscopies in the field of gerontology. The other goal of the present paper is to combine and to compare Raman and FTIR spectroscopic approaches.

2. Experiment

2.1. Subjects

All subjects provided informed consent. The sample set included blood samples (using 4ml Vacutainer tubes containing EDTA) from 74 healthy donors ranging in age from 18 to 87 years (28 males and 46 females) and was subdivided into 10-year age groups (see Table 1). This research was performed, by following the approval by the Ethics Board of the Institute of Gerontology of the NAMS of Ukraine. The blood samples were stored at –20 °C.

Table 1. **Donor information**

Age ranges	Number of samples measured by Raman spectroscopy		Number of samples measured by FTIR spectroscopy	
	Male	Female	Male	Female
18–25	6	3	5	6
26–35	1	6	5	8
36–45	6	6	11	7
46–55	2	4	3	5
56–65	1	5	1	7
66–75	2	3	1	6
76–85	–	2	2	2
86–95	–	–	–	1

2.2. Raman spectroscopy

A self-made Raman microscope in the inverted configuration was used in this research. The system consists of laser sources with wavelengths at 785 nm (diode laser StarBright 785 XM, maximum power 500 mW). Raman spectra were measured via a 40x water immersion objective (Zeiss W Plan-Apochromat 40x/1.0 DIC). The high work distance of the objective (2.5 mm) allowed us to use fused silica window with 1.5-mm thickness between a sample and the immersion liquid. A Princeton Instruments Schmidt–Czerny–Turner spectrograph IsoPlane SCT-320 and a high sensitive CCD PI Pylon 400BR eXcelon cooled with liquid nitrogen were used for the registration of spectra. The spectrograph has a focal length of 320 mm with aperture ratio f/4.6. It was equipped with two gratings, 300 gl/mm (blaze angle 800 nm) and 600 gl/mm (blaze angle 860 nm), which provide the simultaneous measurements of Raman spectra at a laser wavelength of 785 nm in the ranges 200–1900 cm^{-1} and 400–3650 cm^{-1}, respectively.

The blood samples were measured just after thawing. All Raman spectra were measured in the spectral range of 200–1800 cm^{-1} with a spectral resolution of 3 cm^{-1} at the 785-nm excitation wavelength. The laser power was 100 mW in all measurements.

2.3. FTIR spectroscopy

The blood samples were thawing at room temperature, and 100 μL of each sample were dried at room temperature before the measurement (in order to avoid a strong background from water). Reflection spectra in the mid-infrared region (400–4000 cm^{-1}) were registered using a FTIR spectrometer Nicolet iS50 equipped with a single-bounce diamond attenuated total reflection (ATR) accessory. All ATR spectra were measured with a spectral resolution of 4 cm^{-1}. The number of scans for each spectrum was 32.

2.4. Computational details

The PLS analysis of measured FTIR and Raman spectra of human blood was carried out, by using the Themo Scientific TQ Analyst Software.

3. Results

Typical FTIR and Raman spectra of human blood are shown in Fig. 1. The band assignments of IR and Raman spectroscopic signatures of blood are summarized in Table 2.

Information in Table 2 shows that the vibrational spectrum of blood consists of a large number of different vibrational modes from different molecules. It is impossible to analyze such complicated spectrum on the amount of different compounds via simple linear models like Beer's law. Just calibration models like the PLS analysis or principle component regression (PCR) can be used. It is necessary to note that the calibration can be done not only for the determination of a concentration of species in a solution, but it is possible to build the calibration on chemical, biochemical and physical features like the age of donors in our case.

The calibration problem is to establish a quantitative relationship between variables (predictors) $\mathbf{X}$ and response $\mathbf{Y}$, i.e., to construct a mathematical model connecting blocks $\mathbf{X}$ and response $\mathbf{Y}$ [58]. The simplest and widely used calibration model is linear:

$$\mathbf{Y} = \mathbf{XB} + \mathbf{E}. \tag{1}$$

Thus, the aim is to find the matrix $\mathbf{B}$. The simplest way is to use the classical least squares (CLS) approach [58], and $\mathbf{B}$ can be written as

$$\mathbf{B} = (\mathbf{X}^{\mathrm{t}}\mathbf{X})^{-1}\mathbf{X}^{\mathrm{t}}\mathbf{Y}. \tag{2}$$

The main assumption of CLS is the absence of errors in the matrix of predictors $\mathbf{X}$, and errors are present in $\mathbf{Y}$. Another important assumption is the linear independence of predictor vectors $\mathbf{x}_a$. Usually, in spectroscopic applications, the matrix $\mathbf{X}$ contains library spectra of compounds present in the investigated system. The measured spectrum of the sample is not a linear combination of the spectra of pure components due to intermolecular interactions. Moreover, library spectra are not linearly independent in the common case.

The more advanced calibration technique is PCR [58]. First, the matrix $\mathbf{X}$ is decomposed by PCA

$$\mathbf{X} = \mathbf{TP}^{\mathrm{t}} + \mathbf{R}. \tag{3}$$

$\mathbf{T}$ is the so-called score matrix, and $\mathbf{P}$ is the matrix of loadings. The columns of the matrix $\mathbf{T}$ are linearly independent. The obtained score matrix $\mathbf{T}$ is used as a matrix of predictors for further calibration.

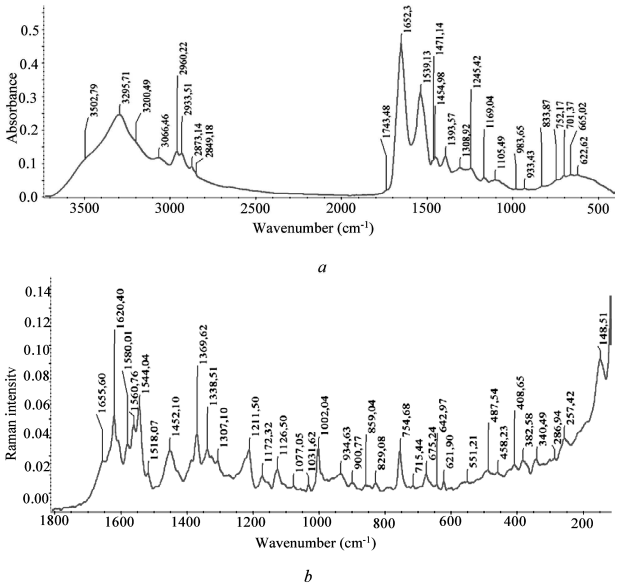

Fig. 1. Typical FTIR (a) and Raman (b) spectra of human blood

Another widely used technique is the PLS regression [58, 59]. The method is similar to PCR. But the principal components in PCR are determined only by the matrix $\mathbf{X}$, while, in PLS, both matrices $\mathbf{X}$ and $\mathbf{Y}$ are used for the determination of principal components. PLS implies the simultaneous PCA decomposition

$$\mathbf{X} = \mathbf{TP}^{\mathrm{t}} + \mathbf{E}, \quad \mathbf{Y} = \mathbf{UQ}^{\mathrm{t}} + \mathbf{F}. \tag{4}$$

These decompositions are performed under the condition of a maximal correlation between the X-score ($\mathbf{t}_a$) and Y-score ($\mathbf{u}_a$) vectors. Therefore, the PLS regression describes much better the complex relationships, by using a smaller number of principal components [60].

Here, we present calibration models which we built according to age-related changes in FTIR and Raman spectra obtained via PLS regression (Fig. 2). In order to perform the PLS analysis, the samples were divided on calibration and validation subsets. After the initial analysis, a few outliers were removed manually. We found correlations with age both for ATR-FTIR (corr. coeff. 0.92) and Raman (corr. coeff. 0.89) spectra of donors' blood. Validation standards were used for testing the calibration accuracy. It is pos-

Table 2. **Assignment of Raman and IR vibrational bands with corresponding literature data**

Wavenumber, cm^{-1}	Bands assignment	IR peak present	Raman peak present
219 (220)	Stretching Fe–His, Mb [15]	–	+
343–345	Stretching Fe–His, deoxy configuration of heme, methemohlobine, Hb [16, 17]	–	+
378	Stretching methemoglobin [16]	+	+
421 (419)	Cholesterol [13, 18] δ (Fe–O–O) [19]	+	–
482	Glycogen, HbO_2 [20, 21, 22, 23]	+	+
524, 527	Stretching S–S in proteins [24], phosphatidylserine [18]	–	+
532 (534)	Cholesterol ester [21, 18]	–	+
559 (565)	Stretching Fe–O_2 [25]	–	+
619–626	Twisting C–C, phenylalanine [24, 26]	+	+
641	Stretching C–S, twist C–C, tyrosine, cysteine, lactose [24, 15, 26]	–	+
660 (662)	Stretching C–S of cysteine, thymine, guanine, adenine in DNA [27, 15]	+	–
674 (672, 673)	Stretching C–S, (pyr. deform.) sym., deoxygenated state of hemoglobin, pyrrole bending (heme) [28, 25, 29, 30]	+	+
680	Symmetric stretching of ferritin (pyr. deform.) [31, 32]	+	+
700	(C–S) trans (aminoacid methionine), cholesterol, cholesterol ester [18, 30]	+	–
747	Thymine in DNA [15]	+	–
754–761	Thymine (ring breathing mode of DNA/RNA bases), DNA, symmetric breathing of tryptophan (protein assignment) [15], stretching pyr. breathing in oxyhemoglobin [9, 19] phosphatidylethanolamine [18], stretching (pyr. breathing) [29, 30]	–	+
825–834	Tyrosine, O–P–O stretch DNA [20, 15]	+	+
858 (854–869)	Tyrosine, proline [20, 21, 30]	–	+
898 (893)	b-D-glucose, fatty acid, phosphodiester, deoxyribose [18, 22, 33, 34]	–	+
935 (934, 933)	C–C stretching mode of proline and valine and protein backbone (α-helix conformation)/glycogen [15, 20]	+	–
976 (977)	CH_3 deformation [15]	–	+
989 (984)	Stretching (C_3N) of porphyrin modes [35]	+	–
1002 (1003, 1004)	Symmetric stretching C–C, phenylalanine [20, 24, 21, 9, 15, 36, 37]	–	+
1023	C–C stretching mode in phospholipids, glycogen [38]	+	–
1029 (1031, 1032)	O–CH_3, stretching of methoxy groups, phenynalanine CH in plane, [20, 24, 15]	+	+
1055	Stretching C–C skeletal, lipid, cholesterol, C–O stretch of glucose region [39, 40, 41]	–	+
1084	C–C stretching (PO_2) in phospholipids an proteins [18, 20, 39, 42, 43]	+	–
1105	Glycogen [44] CO stretching coupled with OH deformation glucose [41, 45, 46]	+	–
1122–1128	C–C stretching in lipids, C–N stretching in proteins, D-mannose, glucose, phospholipid, stretching C-methyl in heme [21, 20, 9, 30]	–	+
1155–1161	C–C (and C–N) stretching of proteins (also carotenoids), glycogen [20, 38, 44, 47, 37]	+	+
1170–1179	C–H in-plane bending mode of tyrosine, C–O ester stretch: cholesterol esters, stretching (pyr. half-ring) asymmetric, C–C, phospholipids, HbO_2 [48, 43, 37]	+	+
1212 (1213, 1211)	C–H deformation in oxyhemoglobin, deoxygenated hemoglobin, asymmetric stretching (PO_2^-) [9, 19, 49]	–	+
1223–1225	Oxygenated state of hemoglobin, – PO_2^- asymmetric stretching vibrations, nucleic acids [25, 42, 50, 37, 30]	+	+

End

Wavenumber, cm^{-1}	Bands assignment	IR peak present	Raman peak present
1243 (1248)	Amide III protein, asymmetric P=O stretching in PO_2, fibrin, asymmetric in plane deformation C–H [48, 43, 51, 36, 30]	+	–
1303–1309 (1300)	Amide III, CH_2 deformation (lipid, adenine) [20, 24, 52, 26]	+	–
1335–1342 (1336)	Amide III, CH_3, CH_2 wagging mode of collagen, glycine, nucleotide chain (DNA-purine bases), fibrin, a1-Acid glycoprotein [20, 21, 39, 52, 36, 37]	+	+
1368–1375	Symmetric stretching (pyr. half-ring), hemoglobin (oxyhemoglobin), methemoglobin, guanine in DNA, tryptophan in proteins, [48, 36, 53, 50] saccharide [18] cholesterol [41]	+	+
1380–1394	CH_3 bending [20]	+	–
1419	Stretching of COO [54], IgG1 [52]	+	–
1439–1445	C–H_2 deformation, tryptophan, collagen, phospholipids, cholesterol [20, 39, 26, 30]	+	
1452 (1456)	CH_2 deformation in lipids, C–H bending in proteins [21, 43]	+	+
1468	C–H bending, CH_2 bending, lipids [43, 55]	+	–
1485 (1482)	Guanine, adenine [15, 26]	+	–
1529 (1526)	–C=C– carotenoid [20, 47]	+	–
1539–1546	Amide II, stretching CN and CNH bending tryptophan, deoxygenated state of hemoglobin, methemoglobin [56, 48, 42, 36, 6]	+	+
1560–1590	Deformation C=C, tryptophan, phenylalanine, acetoacetate, riboflavin, hemoglobin, carboxyhemoglobin, guanine, deoxygenated state of hemoglobin [56, 24, 56, 36, 26, 48]	+	+
1605–1620	C–C stretching of methemoglobin, C=C deoxygenated state of hemoglobin, phenylalanine/tyrosine [16, 24, 36, 26]	+	+
1641–1658	Amide I, C=O hydrogen bonded stretching, hemoglobin (oxygenated state of hemoglobin) [19, 48, 42, 56]	+	–
1660	Amide I proteins, stretching C=C in unsaturated fatty acids [48, 18, 15, 30]	–	+
2863–2865	C–H stretching, Lipids [57]	+	–
2928 (2930)	Fatty acid, cholesterol, CH_2 asymmetric stretching [21, 53, 11]	+	–
2953 (2960)	C–H stretching: CH_2, and CH_3, fatty acid/lipids [43, 54]	+	–
3026 (3015)	Stretching CH of lipids [53]	+	–
3294	Amide A, H-bonded N–H stretching [43]	+	–
3100–3600	Attributed to OH stretch [18, 30]	+	–

"–" – peak is not observed, "+" – peak is present, ( ) – literature data

sible to estimate from Fig. 2 that the vibrational spectra of blood provide the age determination accuracy around ±15 years from FTIR data and around ±20 years from Raman data. Therefore, we can conclude that such calibration models cannot be used for the quantitative analysis of age, but age-related changes really exist and can be obtained from vibrational spectra.

Except calibration models, PLS also provides useful information about Principle Components (PCs), which was built automatically in PLS procedures. Such PC represents spectral curves which independently correlate with age. PCs with the strongest impact into age-related changes obtained from FTIR and Raman data are shown in Fig. 3. It is clearly seen that PC1 curve from FTIR (Fig. 3, *a*) and Raman (Fig. 3, *b*) data very similar to the spectrum of typical protein. This means that the protein (hemoglobin) impact dominates in the vibrational spectrum of blood according to age. Other PCs

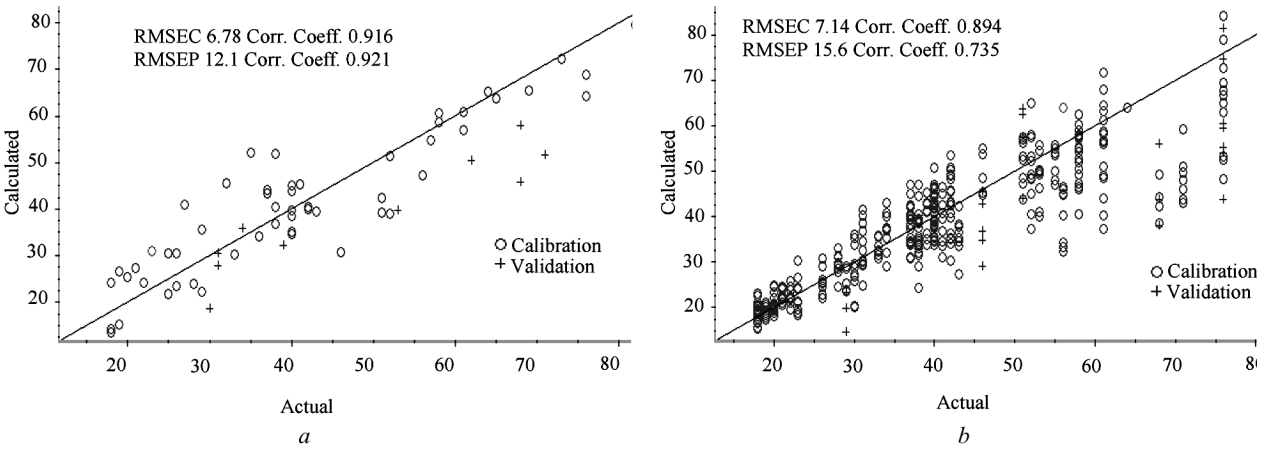

Fig. 2. Calibration models of age-related changes in FTIR (*a*) and Raman (*b*) spectra obtained via PLS regression. RMSEC (Root Mean Square of Calibration), RMSEP (Root Mean Square Error of Prediction)

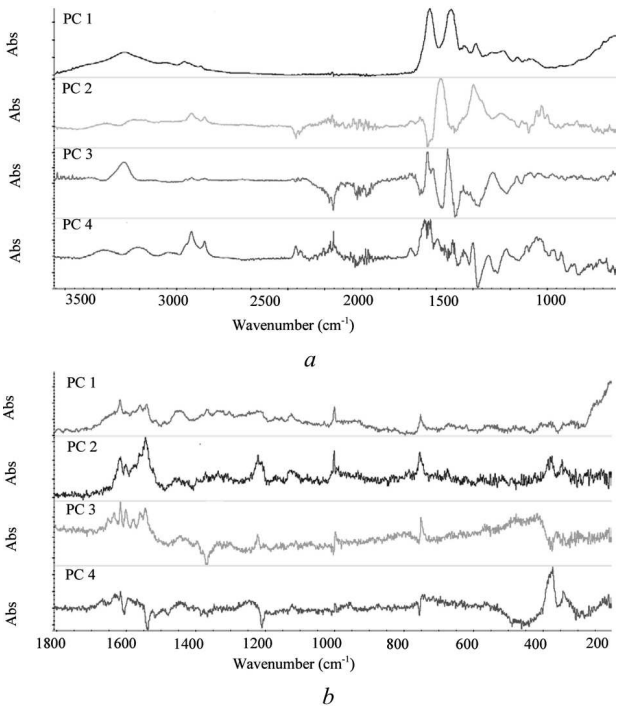

Fig. 3. Derivative principal components of FTIR (*a*) and Raman (*b*) spectra of human blood. PC – principal component

(PC2, PC3, and PC4) can represent theoretically the spectra of different independently correlated chemical compounds according to changes in donor's age. It is seen from the spectra of PC2, PC3, and PC4 that they cannot be interpreted as spectra of blood compounds like albumin, fatty acids, fibrinogen, immunoglobulin, *etc.* First of all, such PCs have negative intensities, which means that non-negative closure constrains was not applied. Therefore, we plan to use chemometric techniques like multivariate curve resolution (MCR) with a possibility of applying the non-negative closure constrains in our future studies. PLS shows that age-related spectral changes are connected with the characteristic ATR-FTIR spectral bands in **PC1** such as at 1640 cm^{-1}, 1525 cm^{-1}, and 1458 cm^{-1} that correspond to hemoglobin, cholesterol, and lipids, respectively; **PC2** has bands at 1587 cm^{-1} (deoxyhemoglobin), 1405 cm^{-1} (immunoglobins), 1023 cm^{-1} (phospholipids); **PC2**: 1298 cm^{-1} (lipids), 1551 cm^{-1} (deoxyhemoglobin), 1653 cm^{-1} (oxyhemoglobin), 3294 cm^{-1}, (Amide A, N–H stretching); **PC4**: 1059 cm^{-1} (phospholipids), 1662 cm^{-1} (fatty acids), 2154 cm^{-1} (not identified), 2367 cm^{-1} (not identified), 2931 cm^{-1} (fatty acids, cholesterol) from FTIR spectra regions (Fig. 3, *a*).

Raman spectra of blood have such bands for each PC – **PC1**: 350 cm^{-1} (deoxyhemoglobin), 379 cm^{-1} (methemoglobin), 754 cm^{-1} (thymine), 1625 cm^{-1} (oxyhemoglobin), 1545 cm^{-1} (methemoglobin), 1005 cm^{-1} (phenylalanine); **PC2**: 358 cm^{-1} (deoxyhemoglobin), 379 cm^{-1} (hemoglobin), 758 cm^{-1} (hemoglobin), 1005 cm^{-1} (phenylalanine), 1224 cm^{-1} (oxyhemoglobin), 1548 cm^{-1} (methemoglobin), 1604 cm^{-1} (deoxyhemoglobin), 1621 cm^{-1} (deoxyhemoglobin), 757 cm^{-1} (hemoglobin), 1002 cm^{-1} (phenylalanine), 1227 cm^{-1} (oxyhemoglobin), 1550 cm^{-1} (deoxyhemoglobin), 1565 cm^{-1} (oxyhemoglobin), 1606 cm^{-1} (deoxyhemo-

globin), 1621 cm^{-1} (deoxyhemoglobin), 1638 cm^{-1} (oxyhemoglobin), 1657 cm^{-1} (oxyhemoglobin) **PC4**: 346 cm^{-1} (deoxyhemoglobin), 376 cm^{-1} (methemoglobin), 758 cm^{-1} (thymine, oxyhemoglobin), 1621 cm^{-1} (oxyhemoglobin).

4. Discussion

The analysis shows that the most spectral changes with age are related to hemoglobin bands alterations. It is known from the study by M. Polakovs *et al.* that irradiation of blood with radioisotopes leads to the transformation of hemoglobin (Fe^{2+}) to methemoglobin (Fe^{3+}) with corresponding changes of Raman spectra in range 1370–1380 cm^{-1} [61]. We found the analogous bands in IR spectra (1377 cm^{-1}) suitable for the age identification. Other authors [53] identified the increasing band 1370 cm^{-1} as a methemoglobin peak, which could be a marker of smoking or some disorders. Comparing this data, we can guess that the hemoglobin transformation is related to age, though disorders also could lead to the same changes in spectra.

The changes observed in the band 2860–3030 cm^{-1} correspond to the age-related lipids content instability. Such lipid modifications with age were explained in [62].

Our further research should be focused on taking samples from larger groups, as well as applying some regression technique to separate contributions from different chemical compounds to the blood spectrum. The dependence of measured spectra on the sample storage time is the other problem to be solved. The studies in forensic sciences demonstrated a significant influence of the storage and exposition time on the spectral properties of blood samples. S. Boyd showed the dependence of the oxyhemoglobin peak intensity on the time passed from the collection [63]. The subsequent possible steps may involve some classic biochemistry methods to support and to verify spectral data.

5. Conclusion

This pilot study has shown the sensitivity of vibrational spectroscopy data to age-related changes in human blood. We have analyzed a set of blood samples from donors of different ages by a combination of Raman and FTIR spectroscopy with the further data processing with Partial Least Squares (PLS) regression. The calibration model of age dependence shows the high values of correlation coefficients both for ATR-FTIR and Raman spectra: 0.92 and 0.89, respectively. Nevertheless, the estimated accuracy of the age determination from FTIR and Raman data is around ± 15 and ± 20 years, respectively. Therefore, we can conclude that such PLS calibration models cannot be used for the precise determination of age, but the age-related changes do really exist and can be detected from vibrational spectra.

1. M.J. Baker, J. Trevisan, P. Bassan, R. Bhargava, H.J. Butler, K.M. Dorling, P.R. Fielden, S.W. Fogarty, N.J. Fullwood, K.A. Heys, C. Hughes, P. Lasch, P.L. Martin-Hirsch, B. Obinaju, G.D. Sockalingum, J. Sulé-Suso, R.J. Strong, M.J. Walsh, B.R Wood, P. Gardner, and F.L Martin, Using Fourier transform IR spectroscopy to analyze biological materials, *Nat. Protoc.* **8**, 1771 (2014) [DOI: 10.1038/nprot.2014.110].
2. D. Naumann, FT-infrared and FT-Raman spectroscopy in biomedical research, *Appl. Spectrosc. Rev.* **36**, 239 (2011) [DOI: 10.1081/ASR-100106157].
3. D.I. Ellis and R. Goodacre, Metabolic fingerprinting in disease diagnosis: biomedical applications of infrared and Raman spectroscopy, *Analyst* **131**, 875 (2006) [DOI: 10.1039/b602376m].
4. S. Yoshida, M. Yoshida, M. Yamamoto, and J. Takeda, Optical screening of diabetes mellitus using non-invasive Fourier-transform infrared spectroscopy technique for human lip, *J. Pharmaceutical and Biomedical Analysis.* **76**, 25, 169 (2013) [DOI: 10.1016/j.jpba.2012.12.009].
5. P.J. Wu, M.H. Chang, C.Y. Huang, Y.C. Wang, J.R. Kuo, Y.J. Huang, and Lin, Near-infrared spectroscopy system for determining brain hemoglobin level, *Conf. Proc. IEEE Eng. Med. Biol. Soc.* **24**, 12 (2013) [DOI: 10.1109/EMBC.2013.6610025].
6. W.R. Premasiri, J.C. Lee, and L.D. Ziegler, Surface-enhanced Raman scattering of whole human blood, blood plasma, and red blood cells: Cellular processes and bioanalytical sensing, *J. Phys. Chem. B* **116**, 9376 (2012) [DOI: 10.1021/jp304932g].
7. B. Yan, B. Li, Z. Wen, X. Luo, L. Xue, and L. Li, Label-free blood serum detection by using surface-enhanced Raman spectroscopy and support vector machine for the preoperative diagnosis of parotid gland tumors, *BMC Cancer* **15**, 650 (2015) [DOI: 10.1186/s12885-015-1653-7].
8. H.M. Heise, R. Marbach, G. Janatsch, and J.D. Kruse-Jarres, Multivariate determination of glucose in whole blood by attenuated total reflection infrared spectroscopy, *Anal. Chem.* **61**, 2009 (1989) [DOI: 10.1021/ac00193a004].
9. S. Ahlawat, A. Chowdhury, N. Kumar, A. Uppal, R.S. Verma, and P.K. Gupta, Polarized Raman spectroscopic investigations on hemoglobin ordering in red blood cells, *J. Biomed. Opt.* **19**, 087002 (2014) [DOI: 10.1117/1.JBO.19.8.087002].

10. P.S. Bernstein, D.-Y. Zhao, S.W. Wintch, I.V. Ermakov, R.W. McClane, and W. Gellermann, Resonance Raman measurement of macular carotenoids in normal subjects and in age-related macular degeneration patients, *Ophthalmology* **109**, 1780 (2002).
11. M. Kozicki, D.J. Creek, A. Sexton, B.J. Morahan, A. Wesełucha-Birczyńska, and B.R. Wood, An attenuated total reflection (ATR) and Raman spectroscopic investigation into the effects of chloroquine on *Plasmodium falciparum*-infected red blood cells, *Analyst* **140**, 2236 (2015) [DOI: 10.1039/C4AN01904K].
12. J.W. Ager, R.K. Nalla, K.L. Breeden, and R.O. Ritchie, Deep-ultraviolet Raman spectroscopy study of the effect of aging on human cortical bone, *J. of Biomed. Opt.* **10**, 034012 (2005) [DOI: 10.1117/1.1924668].
13. K. Virkler and I.K. Lednev, Forensic body fluid identification: the Raman spectroscopic signature of saliva, *Analyst* **135**, 512 (2010) [DOI: 10.1039/b919393f].
14. Y.H. Ong, M. Lim, and Q. Liu, Comparison of principal component analysis and biochemical component analysis in Raman spectroscopy for the discrimination of apoptosis and necrosis in K562 leukemia cells, *Opt. Express* **20**, 22158 (2012) [DOI: 10.1364/OE.20.022158].
15. U. Neugebauer, J.H. Clement, T. Bocklitz, C. Krafft, and J. Popp, Identification and differentiation of single cells from peripheral blood by Raman spectroscopic imaging, *J. Biophoton.* **3**, 579 (2010) [DOI: 10.1002/jbio.201000020].
16. T.G. Spiro and J.M. Burke, Protein control of porphyrin conformation. Comparison of resonance Raman spectra of heme proteins with mesoporphyrin IX analogs, *J. Am. Chem. Soc.* **98**, 5482 (1976) [DOI: 10.1021/ja00434a013].
17. T.W. Scott and J.M. Friedman, Tertiary-structure relaxation in hemoglobin: a transient Raman study, *J. Am. Chem. Soc.* **106**, 5677 (1984) [DOI: 10.1021/ja00331a044].
18. C. Krafft, L. Neudert, T. Simat, and R. Salzer, Near infrared Raman spectra of human brain lipids, *Spectrochim. Acta A: Mol. Biomol. Spectrosc.* **61**, 1529 (2005) [DOI: 10.1016/j.saa.2004.11.017].
19. B.R. Wood, P. Caspers, G.J. Puppels, Sh. Pandiancherri, and D. McNaughton, Resonance Raman spectroscopy of red blood cells using near-infrared laser excitation, *Anal. Bioanal. Chem.* **387**, 1691 (2007) [DOI: 10.1007/s00216-006-0881-8].
20. N. Stone, C. Kendall, J. Smith, P. Crow, and H. Barr, Raman spectroscopy for identification of epithelial cancers, *Faraday Discuss.* **126**, 141 (2004) [DOI: 10.1039/B304992B].
21. L.E. Kamemoto, A.K. Misra, S.K. Sharma, M.T. Goodman, H. Luk, A.C. Dykes, and T. Acosta, Near-infrared micro-Raman spectroscopy for in vitro detection of cervical cancer, *Appl. Spectrosc.* **64**, 255 (2010) [DOI: 10.1366/000370210790918364].
22. G. Shetty, C. Kedall, N. Shepherd, N. Stone, and H. Barr, Raman spectroscopy: elucidation of biochemical changes in carcinogenesis of oesophagus, *Br. J. Cancer* **94**, 1460 (2006) [DOI: 10.1038/sj.bjc.6603102].
23. L. Rimai, I. Salmeen, and D.H. Petering, Comparison of the resonance Raman spectra of carbon monoxy and oxy hemoglobin and myoglobin: similarities and differences in heme electron distribution, *Biochemistry* **14**, 378 (1975).
24. J. Lin, R. Chen, S. Feng, J. Pan, Y. Li, G. Chen, M. Cheng, Z. Huang, Y. Yu, and H. Zeng, A novel blood plasma analysis technique combining membrane electrophoresis with silver nanoparticle-based SERS spectroscopy for potential applications in noninvasive cancer detection, *Nanomedicine: Nanotechnology, Biology, and Medicine* **7**, 655 (2011) [DOI: 10.1016/j.nano.2011.01.012].
25. A. Bankapur, S. Barkur, S. Chidangil, and D. Mathur, A micro-Raman study of live, single red blood cells (RBCs) treated with $AgNO_3$ nanoparticles, *PLoS One* **9**, e103493 (2014) [DOI: 10.1371/journal.pone.0103493].
26. J.W. Chan, D.S. Taylor, T. Zwerdling, S.M. Lane, K. Ihara, and T. Huser, Micro-Raman spectroscopy detects individual neoplastic and normal hematopoietic cells, *Biophys. J.* **90**, 648 (2006) [DOI: 10.1529/biophysj.105.066761].
27. B. Prescott, W. Steinmetz, and G.J. Thomas, Characterization of DNA structures by laser Raman spectroscopy, *Biopolymers* **23**, 235 (1984) [DOI: 10.1002/bip.360230206].
28. T.G. Spiro and T.C. Strekas, Resonance Raman spectra of heme proteins. Effects of oxidation and spin state, *J. Am. Chem. Soc.* **96**, 338 (1974) [DOI: 10.1021/ja00809a004].
29. B.R. Wood and D. McNaughton, Raman excitation wavelength investigation of single red blood cells *in vivo*, *J. Raman Spectrosc.* **33**, 517 (2002) [DOI: 10.1002/jrs.870].
30. C. Krafft, S.B. Sobottka, G. Schackertb, and R. Salzer, Near infrared Raman spectroscopic mapping of native brain tissue and intracranial tumors, *Analyst* **130**, 1070 (2005) [DOI: 10.1039/b419232j].
31. W. Chua-anusorn and J. Webb, Infrared spectroscopic studies of nanoscale iron oxide deposits isolated from human thalassemic tissues, *J. Inorg. Biochem.* **79**, 303 (2000) [DOI: 10.1016/S0162-0134(99)00233-0].
32. G. Rusciano, A. De Luca, G. Pesce, and A. Sasso, Raman tweezers as a diagnostic tool of hemoglobin-related blood disorders, *Sensors* **8**, 7818 (2008) [DOI: 10.3390/s8127818].
33. A.J. Ruiz-Chica, M.A. Medina, F. Sánchez-Jiménez, and F.J. Ramírez, Characterization by Raman spectroscopy of conformational changes on guanine–cytosine and adenine–thymine oligonucleotides induced by aminooxy analogues of spermidine, *J. Raman Spectrosc.* **35**, 93 (2004) [DOI: 10.1002/jrs.1107].
34. V.K. Ghodakel and G.R. Kulkarnil, Effect of low frequency mechanical vibrations on human blood (in vitro), *Int. J. Chem. Phys. Sci.* **4** Special Issue 5 ETP (2015).
35. L.N. Salmaso, G.J. Puppels, P.J. Caspers, R. Floris, R. Wever, and J. Greve, Resonance Raman microspectroscopic characterization of eosinophil peroxidase in human eosinophilic granulocytes, *Biophys. J.* **67**, 436 (1994) [DOI: 10.1016/S0006-3495(94)80499-0].
36. N. Stone, C. Kendell, N. Shepherd, P. Crow, and H. Barr, Near-infrared Raman spectroscopy for the classification of

epithelial pre-cancers and cancers, *J. Raman Spectrosc.* **33**, 564 (2002) [DOI: 10.1002/jrs.882].
37. Z. Huang, A. McWclliams, H. Lui, D.I. McLean, S. Lam, and H. Zeng, Near-infrared Raman spectroscopy for optical diagnosis of lung cancer, *Int. J. Cancer* **107**, 1047 (2003) [DOI: 10.1002/ijc.11500].
38. A. Mahadevan-Jansen and R.R. Kortum, Raman spectroscopy for the detection of cancers and precancers, *J. Biomed. Opt.* **1**, 31 (1996) [DOI: 10.1117/12.227815].
39. R.K Dukor, Vibrational spectroscopy in the detection of cancer, *Biomed. Appl.* **5**, 3335 (2002).
40. J.V. Glenn, J.R. Beattie, L. Barrett, N. Frizzell, S.R. Thorpe, M.E. Boulton, J.J. McGarvey, and A.W. Stitt, Confocal Raman microscopy can quantify advanced glycation end product (AGE) modifications in Bruch's membrane leading to accurate, nondestructive prediction of ocular aging, *The FASEB Journal* **21**, 3542 (2007) [DOI: 10.1096/fj.06-7896com].
41. G. Budínová, J. Salva, and K. Volka, Application of molecular spectroscopy in the mid-infrared region to the determination of glucose and cholesterol in whole blood and in blood serum, *Appl. Spectrosc.* **51**, 631 (1997) [DOI: 10.1366/0003702971941034].
42. S. Olsztyńska-Janus, K. Szymborska-Małek, M. Gąsior-Głogowska, T. Walski, M. Komorowska, W. Witkiewicz, C. Pezowicz, M. Kobielarz, and S. Szotek, Spectroscopic techniques in the study of human tissues and their components. Part I: IR spectroscopy, *Acta of Bioengin. and Biomech. Rev.* **14**, 101 (2012) [DOI: 10.5277/abb120314].
43. R. Manoharan, J.J. Baraga, R.P. Rava, R.R. Dasari, M. Fitzmaurice, and M.S. Feld, Biochemical analysis and mapping of atherosclerotic human artery using FT-IR microspectroscopy, *Atherosclerosis* **103**, 181 (1993) [DOI: 10.1016/0021-9150(93)90261-R].
44. N.S. Eikje, K. Aizawa, T. Sota, Y. Ozaki, and S. Arase, Identification and characterization of skin biomolecules for drug targeting and monitoring by vibrational spectroscopy, *Open Med. Chem. J.* **2**, 38 (2008) [DOI: 10.2174/1874104500802010038].
45. Y.-J. Kim, S. Hahn, and G. Yoon, Determination of glucose in whole blood samples by mid-infrared spectroscopy, *Appl. Opt.* **42**, 745 (2003) [DOI: 10.1364/AO.42.000745].
46. L.A. Tamic and K.A. Hartman, The infrared spectra and structure of the amadori product formed from glucose and glycine, *Appl. Spectrosc.* **39**, 591 (1985) [DOI: 10.1366/0003702854250095].
47. S. Arikana, H.S. Sands, R.G. Rodwaya, and D.N. Batchelder, Raman spectroscopy and imaging of β-carotene in live corpus luteum cells, *Animal Reprod. Sci.* **71**, 249 (2002) [DOI: 10.1016/S0378-4320(02)00020-9].
48. M.F. Zhu, X.P. Ye, Y.Y. Huang, Z.Y. Guo, Z.F. Zhuang, and S.H. Liu, Detection of methemoglobin in whole blood based on confocal micro-Raman spectroscopy and multivariate statistical techniques, *Scanning* **36**, 471 (2014) [DOI: 10.1002/sca.21143].
49. S. Olsztyńska-Janus, M. Gąsior-Głogowska, K. Szymborska-Małek, B. Czarnik-Matusewicz, and M. Komorowska, Specific applications of vibrational spectroscopy in biomedical engineering, *Biomedical Engineering, Trends, Research and Techn.* **4**, 91 (2011) [DOI: 10.5772/13121].
50. B.R. Wood, P. Caspers, G.J. Puppels, Sh. Pandiancherri, and D. McNaughton, Resonance Raman spectroscopy of red blood cells using near-infrared laser excitation, *Anal. Bioanal. Chem.* **387**, 1691 (2007) [DOI: 10.1007/s00216-006-0881-8].
51. D. Sheng, Y. Wu, X. Wang, D. Huang, X. Chen, and X. Liu, Comparison of serum from gastric cancer patients and from healthy persons using FTIR spectroscopy, *Spectrochim. Acta Part A: Mol. and Biomol. Spectr.* **116**, 365 (2013) [DOI: 10.1016/j.saa.2013.07.055].
52. C. Petibois, G. Cazorla, A. Cassaigne, and G. Déléris, Plasma protein contents determined by Fourier-transform infrared spectrometry, *Clinical Chemistry* **47**, 730 (2001).
53. M. Polakovs, N. Mironova-Ulmanea, N. Kurjaneb, E. Reinholdsc, and M. Grubed, *Proc. of Sixth International Conference on Advanced Optical Materials and Devices*, edited by J. Spigulis, A. Krumins, D. Millers, A. Sternberg, I. Muzikante, A. Ozols, M. Ozolinsh, SPIE (2008) p. 714214-1.
54. S.J. Ahmed, W. Santosh, S. Kumar *et al.*, Neural network algorithm for the early detection of Parkinson's disease from blood plasma by FTIR micro-spectroscopy, *Vib. Spectrosc.* **53**, 181 (2010) [DOI: 10.1016/j.vibspec.2010.01.019].
55. Changan Xie and Yong-qing Li, Confocal micro-Raman spectroscopy of single biological cells using optical trapping and shifted excitation difference techniques, *J. Appl. Phys.* **93**, 2982 (2003) [DOI: 10.1063/1.1542654].
56. T.C. Strecas and T.G. Spiro, Hemoglobin: Resonance Raman spectra, *Biochim. Biophys. Acta* **263**, 830 (1972) [DOI: 10.1016/0005-2795(72)90072-4].
57. A. Perrenoud, E.C. Rangel, R.P. Mota, S.F. Durrant, and N.C. da Cruz, Evaluation of blood compatibility of plasma deposited heparin-like films and SF6 plasma treated surfaces, *Mat. Res.* **13**, 95 (2010) [DOI: 10.1590/S1516-14392010000100019].
58. A.L. Pomerantsev, *Chemometrics in Excel* (Wiley, New York, 2014).
59. P.H. Garthwaite, An interpretation of partial least squares, *J. Am. Stat. Assoc.* **89**, 122 (1994) [DOI: 10.2307/2291207].
60. O.Ye. Rodionova and A.L. Pomerantsev, Chemometrics: achievements and prospects, *Russ. Chem. Rev.* **75**, 271 (2006) [DOI: 10.1070/RC2006v075n04ABEH003599].
61. B.R. Wood, B. Tait, and D. McNaughton, Micro-Raman characterisation of the R to T state transition of haemoglobin within a single living erythrocyte, *Biochim. Biophys. Acta* **1539**, 58 (2001).
62. W.F. DeNino, A. Tchernof, I.J. Dionne, M.J. Toth, P.A. Ades, C.K. Sites, and E.T. Poehlman, Contribution of abdominal adiposity to age-related differences in insulin sensitivity and plasma lipids in healthy nonobese women, *Diabetes Care* **24**, 925 (2001).

63. S. Boyd, M.F. Bertino, and S.J. Seashols, Raman spectroscopy of blood samples for forensic applications, *Forensic Sci. Intern.* **208**, 124 (2011) [DOI: 10.1016/j.forsciint.2010.11.012].

Received 05.04.16

Т. Махній, О. Ільченко, А. Рейнт, Ю. Пільгун, А. Куцик, Д. Красненков, М. Івасюк, В. Кухарський

ВІК-ЗАЛЕЖНІ ЗМІНИ РАМАН- ТА ІЧ-СПЕКТРІВ КРОВІ ЛЮДИНИ

Р е з ю м е

Розглянуто можливості застосування Раман- та ІЧ-спектроскопії для аналізу вікових змін крові людини. Досліджено 74 зразки крові пацієнтів різних вікових груп. До досліджуваних спектрів було застосовано PLS-аналіз. Виявлено недостатню точність методу для визначення віку. При цьому були знайдені вік-залежні ділянки спектрів. Було охарактеризовано основні ділянки спектрів, що показали зміни, залежні від віку, відповідно до PLS-аналізу та літературних даних. В статті наведено приклади характерних Раман- та ІЧ-спектрів. Значення всіх знайдених піків Раман- та ІЧ-спектрів зібрані та описані у таблиці відповідно до літературних даних. Знайдено, що основні відмінності стосуються піків, які несуть інформацію про гемоглобін та його похідні. Було зроблено висновок щодо необхідності проведення досліду з більшою кількістю зразків.